

# Synthesis, Structure, and Thermophysical Properties of $\text{Pb}_{10-x}\text{Bi}_x(\text{GeO}_4)_2+x(\text{VO}_4)_{4-x}$ ( $x = 0-3$ ) in the Temperature Range of 350–950 K

L. T. Denisova<sup>a,\*</sup>, M. S. Molokeev<sup>b,c</sup>, V. M. Denisov<sup>a</sup>,  
E. O. Golubeva<sup>a</sup>, and N. A. Galiakhmetova<sup>a</sup>

<sup>a</sup> Siberian Federal University, Institute of Metallurgy and Materials Science, Krasnoyarsk, 660041 Russia

<sup>b</sup> Siberian Federal University, Institute of Engineering Physics and Radio Electronics, Krasnoyarsk, 660041 Russia

<sup>c</sup> Kirensky Institute of Physics, Krasnoyarsk Scientific Center, Siberian Branch,  
Russian Academy of Sciences, Krasnoyarsk, 660036 Russia

\*e-mail: antluba@mail.ru

Received July 4, 2020; revised July 4, 2020; accepted July 8, 2020

**Abstract**—The  $\text{Pb}_{10-x}\text{Bi}_x(\text{GeO}_4)_2+x(\text{VO}_4)_{4-x}$  ( $x = 0-3$ ) compounds with an apatite structure have been obtained for the first time from the initial  $\text{PbO}$ ,  $\text{Bi}_2\text{O}_3$ ,  $\text{GeO}_2$ , and  $\text{V}_2\text{O}_5$  oxides by the solid-state synthesis in the temperature range of 773–1073 K. The structure of the compounds has been determined by X-ray diffraction analysis. The effect of temperature on specific heat of the synthesized compounds has been investigated by differential scanning calorimetry. The thermodynamic properties of the compounds have been calculated from the experimental  $C_p = f(T)$  data.

**Keywords:** bismuth-doped lead vanadate germanates, apatites, structure, high-temperature specific heat, thermodynamic properties

**DOI:** 10.1134/S1063783420110116

## 1. INTRODUCTION

The  $\text{M}_{10}(\text{ZO}_4)_6\text{X}_2$  ( $\text{M} = \text{Ca}, \text{Ba}, \text{Pb}, \text{etc.}; \text{Z} = \text{P}, \text{As}, \text{V}, \text{Si}, \text{Ge}, \text{etc.}; \text{X} = \text{OH}, \text{F}, \text{Cl}, \text{Br}, \text{J}, \text{O}, \text{etc.}$ ) compounds with an apatite structure have attracted attention of researchers and practitioners for a long time [1–9]. This is due to the unique properties for application. They are used as biomaterials, sensors, phosphors, laser and fluorescent materials, and catalysts [10–12]. A feature of the compounds with an apatite structure is the ability of their structural units to be replaced by other ions. In particular, replacing lead in the  $\text{Pb}_5(\text{GeO}_4)(\text{VO}_4)_2$  apatite by rare-earth elements makes it possible to obtain the  $\text{Pb}_{10-x}\text{R}_x(\text{GeO}_4)_2+x(\text{VO}_4)_{4-x}$  ( $\text{R} = \text{REE}, x = 0-3$ ) compounds with the same structure [9, 13]. The crystal structure of apatites belongs to the hexagonal syngony, sp. gr.  $P6_3/m$  [7, 11, 14]. They are characterized by the presence of two structurally nonequivalent sites ( $M1$ ) and ( $M2$ ) in the cationic sublattice. In searching for new materials with such properties, it was believed that the replacement of lead by  $\text{Bi}^{3+}$  in the  $\text{Pb}_5(\text{GeO}_4)(\text{VO}_4)_2$  compound would yield  $\text{Pb}_{10-x}\text{Bi}_x(\text{GeO}_4)_2+x(\text{VO}_4)_{4-x}$  ( $x = 1-3$ ) with an apatite structure. Such compounds have not been obtained and their structure and properties have not been studied.

In this work, we report on the results of the synthesis and investigations of the structure and thermophysical properties of the  $\text{Pb}_{10-x}\text{Bi}_x(\text{GeO}_4)_2+x(\text{VO}_4)_{4-x}$  ( $x = 1-3$ ) compounds.

## 2. EXPERIMENTAL

The  $\text{Pb}_{10-x}\text{Bi}_x(\text{GeO}_4)_2+x(\text{VO}_4)_{4-x}$  ( $x = 1-3$ ) powders were synthesized by the solid-state synthesis from the  $\text{PbO}$ ,  $\text{Bi}_2\text{O}_3$ , and  $\text{V}_2\text{O}_5$  (extra pure grade) and  $\text{GeO}_2$  (99.999%). For this purpose, stoichiometric mixtures of the pre-calcined oxides were ground in an agate mortar, tableted, and burnt in air at temperatures of 773, 873, 973, and 1073 K for 10 h. Note that, at the latter temperature, the samples with  $x = 2, 3$  slightly melted. To ensure the completeness of the solid-state reaction, after burning at each temperature, the samples were ground and pressed again. The phase composition of the obtained samples was controlled by X-ray diffraction analysis. Room-temperature X-ray powder diffraction patterns of the  $\text{Pb}_{10-x}\text{Bi}_x(\text{GeO}_4)_2+x(\text{VO}_4)_{4-x}$  ( $x = 1-3$ ) apatites (the data on the structure of the  $\text{Pb}_5(\text{GeO}_4)(\text{VO}_4)_2$  ( $x = 0$ ) compound were obtained in [2]) were obtained on a Bruker D8 ADVANCE diffractometer ( $\text{CuK}\alpha$  radi-

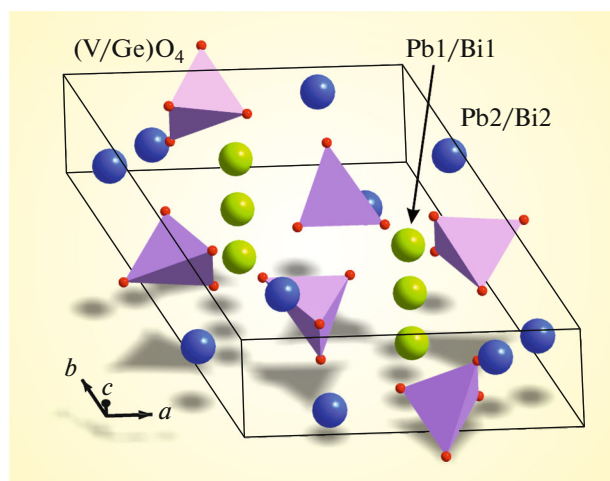


Fig. 1.  $\text{Pb}_{10-x}\text{Bi}_x(\text{GeO}_4)_2+x(\text{VO}_4)_{4-x}$  crystal structure.

tion) using a VANTEC linear detector. The scanning step was  $0.016^\circ$  and the exposure time was 2 s at each step. The Rietveld refinement was performed using the TOPAS 4.2 software [15].

The specific heat of the  $\text{Pb}_{10-x}\text{Bi}_x(\text{GeO}_4)_2+x(\text{VO}_4)_{4-x}$  apatite was measured on an STA 449 C Jupiter thermal analyzer (NETZSCH, Germany). The experimental technique is similar to that described in [16]. The experimental error was no more than 2%.

### 3. RESULTS AND DISCUSSION

It was established that the  $\text{Pb}_{10-x}\text{Bi}_x(\text{GeO}_4)_2+x(\text{VO}_4)_{4-x}$  ( $x = 1-3$ ) crystal structure is isostructural to the  $\text{Pb}_{10}(\text{GeO}_4)_2(\text{VO}_4)_4$  compound, the structure of

which was determined in [2, 9, 17]. Therefore, the structure of this crystal is taken as a starting model for the refinement. To transform the structure, Pb/Bi ions were placed in both independent sites (Pb1) and (Pb2) of lead ions (Fig. 1). For a single Ge/V site, the ionic ratio Ge : V was calculated taking into account the proposed chemical formula. Further, their populations were fixed during the refinements. The thermal parameters of all atoms were refined in the isotropic approximation. The refinement was stable and yielded the small  $R$  factors (Table 1, Fig. 2). The atomic coordinates and basic bond lengths are given in Tables 2 and 3, respectively.

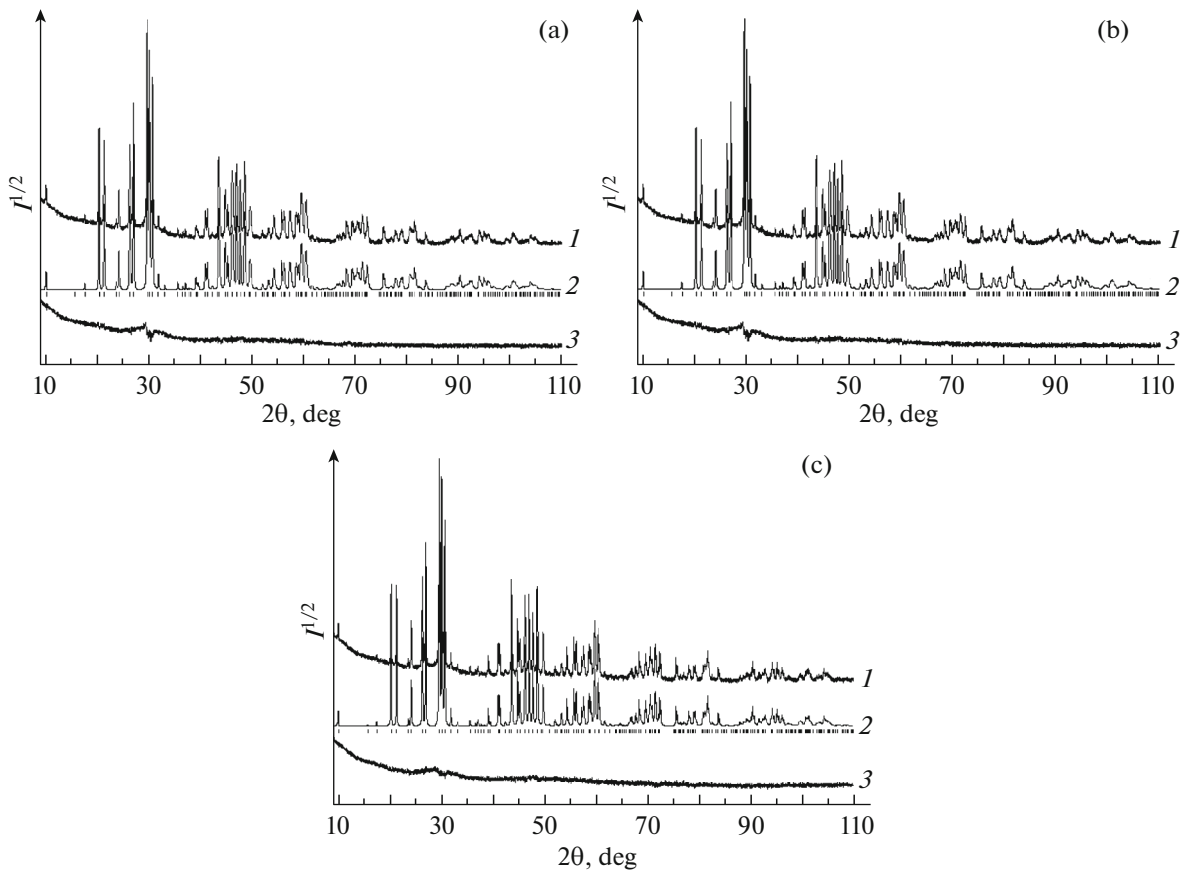
The effect of substitution of bismuth for lead in  $\text{Pb}_{10-x}\text{Bi}_x(\text{GeO}_4)_2+x(\text{VO}_4)_{4-x}$  on the parameters of the unit cell is illustrated in Fig. 3. It can be seen that, with an increase in the bismuth concentration, all the cell parameters ( $a$ ,  $c$ ,  $V$ ) decrease, while the density increases. A decrease in the cell volume with the increasing bismuth content is consistent with the smaller ionic radius of  $\text{Bi}^{3+}$  as compared with that of the  $\text{Pb}^{2+}$  ion and confirms that the proposed chemical formulas for the three compounds are similar to reality.

Figure 4 shows the effect of temperature on the specific heat of the  $\text{Pb}_{10-x}\text{Bi}_x(\text{GeO}_4)_2+x(\text{VO}_4)_{4-x}$  ( $x = 1-3$ ) apatite. For comparison, the data on  $\text{Pb}_{10}(\text{GeO}_4)_2(\text{VO}_4)_4$  obtained by us previously [18] are presented. It can be seen that, as the temperature increases, the  $C_p$  values for all the investigated apatite compositions regularly increase and the  $C_p = f(T)$  curves contain no different extrema. This is apparently due to the fact that these compounds do not undergo polymorphic transformations in the investigated temperature range. In addition, with an increase in the

Table 1. Main parameters of the shot and refinement of the  $\text{Pb}_{10-x}\text{Bi}_x(\text{GeO}_4)_2+x(\text{VO}_4)_{4-x}$  crystal structure

$x$	1	2	3
Sp. Gr	$P6_3/m$	$P6_3/m$	$P6_3/m$
$a$ , Å	10.08657(6)	10.0802(2)	10.0624(1)
$c$ , Å	7.37010(6)	7.3512(2)	7.3154(1)
$V$ , Å <sup>3</sup>	649.369(9)	646.88(3)	641.46(1)
$d$ , g/cm <sup>3</sup>	7.230	7.319	7.438
$Z$	1	1	1
2 $\theta$ -interval, deg	10–120	10–120	10–120
$R_{wp}$ , %	5.63	6.03	6.46
$R_p$ , %	4.40	4.75	5.08
$R_{exp}$ , %	3.80	3.08	3.30
$\chi^2$	1.48	1.96	1.96
$R_B$ , %	2.08	1.53	2.47

$a$ ,  $c$ , and  $\beta$  are the cell parameters,  $V$  is the cell volume, and  $d$  is the calculated density. The infidelity factors are weight profile  $R_{wp}$ , profile  $R_p$ , expected  $R_{exp}$ , integral  $R_B$ , and fitting quality  $\chi^2$ .



**Fig. 2.** (1) Experimental, (2) calculated, and (3) difference profiles of  $\text{Pb}_{10-x}\text{Bi}_x(\text{GeO}_4)_2+x(\text{VO}_4)_{4-x}$  ( $x =$  (a) 1, (b) 2, and (c) 3) after the Rietveld refinement. Marks show the calculated reflection positions.

bismuth content, the specific heat capacity of the  $\text{Pb}_{10-x}\text{Bi}_x(\text{GeO}_4)_2+x(\text{VO}_4)_{4-x}$  apatites also increases (Fig. 3).

It was established that the temperature dependences of the specific heat of the investigated compounds are described by the equation [19]

$$C_p = a + bT + cT^{-2} + dT^2, \quad (1)$$

which describes the experimental specific heat values better than the Maier–Kelley equation [20]

$$C_p = a + bT + cT^{-2}. \quad (2)$$

Note that the same was observed for the  $\text{Pb}_8\text{La}_2(\text{GeO}_4)_4(\text{VO}_4)_2$  apatite [21]. This behavior of the specific heat for  $\text{Pb}_{10-x}\text{Bi}_x(\text{GeO}_4)_2+x(\text{VO}_4)_{4-x}$  at high temperatures is apparently due to the fact that, upon approaching the melting point, the specific heat of solids anomalously grows [22]. For instance, according to [1], the melting point of the  $\text{Pb}_{10}(\text{GeO}_4)_2(\text{VO}_4)_4$  apatite is 1178 K. We found that, for  $\text{Pb}_8\text{Bi}_2(\text{GeO}_4)_4(\text{VO}_4)_2$  and  $\text{Pb}_7\text{Bi}_3(\text{GeO}_4)_5(\text{VO}_4)$ , they are equal to 1013 K.

Equation (1) for the investigated  $\text{Pb}_{10-x}\text{Bi}_x(\text{GeO}_4)_2+x(\text{VO}_4)_{4-x}$  apatites has the form

$$x = 1:$$

$$C_p = (1024.5 \pm 22.92) - (189.6 \pm 49.2) \times 10^{-3}T \quad (3) \\ - (120.5 \pm 12.64) \times 10^5 T^{-2} + (24.77 \pm 2.83) \times 10^{-5} T^2,$$

$$x = 2:$$

$$C_p = (1113.5 \pm 32.84) - (388.4 \pm 72.6) \times 10^{-3}T \quad (4) \\ - (161.0 \pm 17.31) \times 10^5 T^{-2} + (42.93 \pm 4.32) \times 10^{-5} T^2,$$

$$x = 3:$$

$$C_p = (1045.8 \pm 49.89) - (233.9 \pm 11.1) \times 10^{-3}T \quad (5) \\ - (125.2 \pm 26.06) \times 10^5 T^{-2} + (39.17 \pm 6.66) \times 10^{-5} T^2.$$

The correlation coefficients for Eqs. (3)–(5) are 0.9986, 0.9986, and 0.9978, respectively. Using these equations, the thermodynamic functions of the investigated apatites were calculated from the known thermodynamic relations. The results are given in Table 4 (these data for the unsubstituted  $\text{Pb}_{10}(\text{GeO}_4)_2(\text{VO}_4)_4$  apatite were obtained by us in [18]).

**Table 2.** Atomic coordinates and isotropic heat parameters (Å) of the  $\text{Pb}_{10-x}\text{Bi}_x(\text{GeO}_4)_2+x(\text{VO}_4)_{4-x}$  crystals

Atom	$x$	$y$	$z$	$B_{\text{iso}}$	$Occ$
$x = 1$					
Pb1	1/3	2/3	0.0060(5)	1.45(7)	0.981(45)
Bi1	1/3	2/3	0.0060(5)	1.45(7)	0.019(45)
Pb2	0.25335(15)	0.0016(3)	0.25	1.37(7)	0.848(30)
Bi2	0.25335(15)	0.0016(3)	0.25	1.37(7)	152(30)
Ge	0.3989(4)	0.3821(4)	0.25	0.30(10)	1/2
V	0.3989(4)	0.3821(4)	0.25	0.30(10)	1/2
O1	0.3036(18)	0.4802(18)	0.25	3.2(3)	1
O2	0.5897(17)	0.4934(16)	0.25	3.2(3)	1
O3	0.3582(12)	0.2599(12)	0.0635(13)	3.2(3)	1
$x = 2$					
Pb1	1/3	2/3	0.0065970	2.00(9)	0.60(12)
Bi1	1/3	2/3	0.0065(7)	2.00(9)	0.40(12)
Pb2	0.25458(19)	0.0030(3)	0.25	1.90(9)	0.90(12)
Bi2	0.25458(19)	0.0030(3)	0.25	1.90(9)	0.10(12)
Ge	0.3951(5)	0.3815(5)	0.25	0.44(12)	2/3
V	0.3951(5)	0.3815(5)	0.25	0.44(12)	1/3
O1	0.303(2)	0.483(2)	0.25	4.3(4)	1
O2	0.5786(19)	0.5037(19)	0.25	4.3(4)	1
O3	0.3528(14)	0.2590(14)	0.0631(17)	4.3(4)	1
$x = 3$					
Pb1	1/3	2/3	0.0058(8)	2.13(10)	0.40(17)
Bi1	1/3	2/3	0.0058(8)	2.13(10)	0.60(17)
Pb2	0.2545(2)	0.0021(4)	0.25	1.68(10)	0.88(12)
Bi2	0.2545(2)	0.0021(4)	0.25	1.68(10)	0.12(12)
Ge	0.3973(6)	0.3846(6)	0.25	0.30(13)	5/6
V	0.3973(6)	0.3846(6)	0.25	0.30(13)	1/6
O1	0.317(3)	0.500(3)	0.25	5.1(5)	1
O2	0.574(2)	0.499(2)	0.25	5.1(5)	1
O3	0.3587(18)	0.2560(17)	0.069(2)	5.1(5)	1

We could not compare our data with results of other authors due to their lack. However, this can be made using the additive Neumann–Kopp method [23–25]

$$C_{p298}(j) = \sum_i C_{p298}(i), \quad (6)$$

where  $C_{p298}(j)$  is the molar specific heat of the complex oxide compound,  $C_{p298}(i)$  is the molar specific heat of the  $i$ th simple oxide, and  $m_i$  is the molar fraction of the corresponding simple oxide. It was found

that the  $C_p$  values calculated using Eq. (6) for the investigated apatites are lower than the experimental values by 4.2, 4.5, and 6.7% for  $x = 1, 2,$  and  $3,$  respectively. According to [22], the positive or negative deviations from the Neumann–Kopp additive rule are related to the changes in the vibration frequencies of atoms in the complex oxide compound as compared with the simple oxides. The  $C_{p298}(i)$  values for  $\text{PbO}, \text{Bi}_2\text{O}_3, \text{GeO}_2,$  and  $\text{V}_2\text{O}_5$  required for the calculation using Eq. (6) were taken from [24]. The same devia-

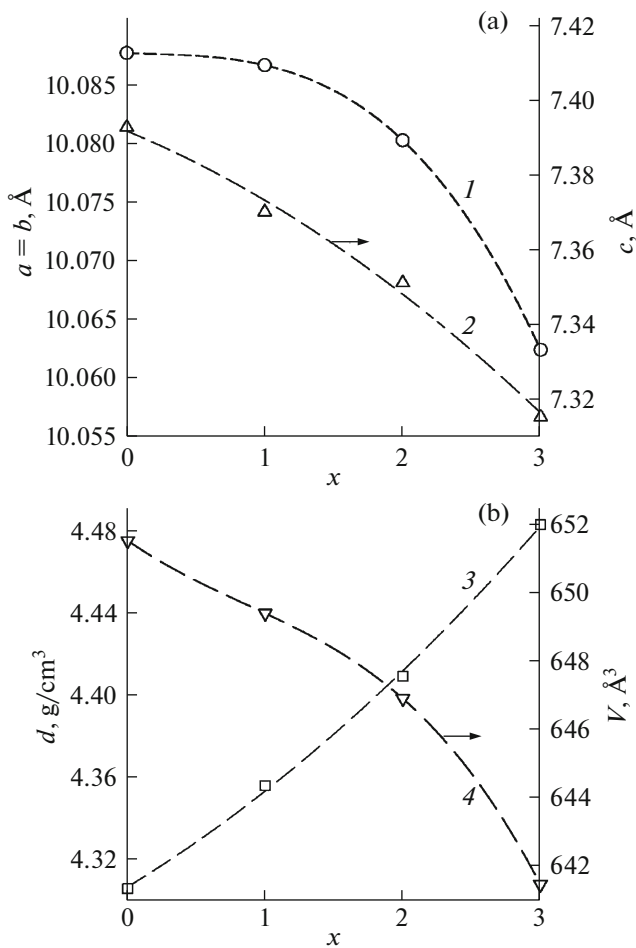


**Fig. 3.** Effect of the  $\text{Pb}_{10-x}\text{Bi}_x(\text{GeO}_4)_2+x(\text{VO}_4)_{4-x}$  apatite composition on the unit cell parameters. (1)  $a = b$ , (2)  $c$ , (3)  $d$ , and (4)  $V$ .

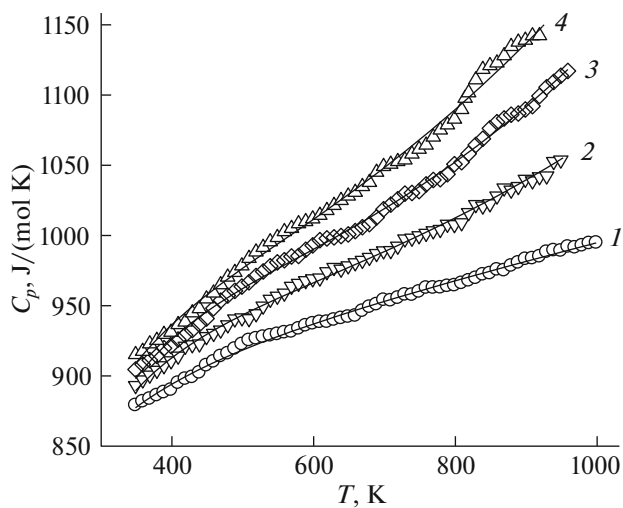


**Fig. 4.** Effect of temperature on the molar specific heat of  $\text{Pb}_{10-x}\text{Bi}_x(\text{GeO}_4)_2+x(\text{VO}_4)_{4-x}$  ( $x = (1) 0, (2) 1, (3) 2,$  and (4) 3).

**Table 3.** Main bond lengths (Å) in the  $\text{Pb}_{10-x}\text{Bi}_x(\text{GeO}_4)_2+x(\text{VO}_4)_{4-x}$  crystals

$x = 1$			
(Pb1/Bi1)—O1	2.509(11)	(GeV)—O1	1.690(11)
(Pb1/Bi1)—O2 <sup>i</sup>	2.833(11)	(Ge/V)—O2	1.674(11)
(Pb1/Bi1)—O3 <sup>i</sup>	2.861(10)	(Ge/V)—O3	1.752(10)
(Pb2/Bi2)—O1 <sup>ii</sup>	2.774(15)		
(Pb2/Bi2)—O2 <sup>iii</sup>	2.236(14)		
(Pb2/Bi2)—O3	2.653(10)		
(Pb2/Bi2)—O3 <sup>iv</sup>	2.535(10)		
$x = 2$			
(Pb1/Bi1)—O1	2.484(14)	(Ge/V)—O1	1.687(14)
(Pb1/Bi1)—O2 <sup>i</sup>	2.969(13)	(Ge/V)—O2	1.631(14)
(Pb1/Bi1)—O3 <sup>i</sup>	2.909(12)	(Ge/V)—O3	1.751(13)
(Pb2/Bi2)—O1 <sup>ii</sup>	2.79(2)		
(Pb2/Bi2)—O2 <sup>iii</sup>	2.167(17)		
(Pb2/Bi2)—O3	2.641(12)		
(Pb2/Bi2)—O3 <sup>iv</sup>	2.509(12)		
$x = 3$			
(Pb1/Bi1)—O1	2.402(16)	(GeV)—O1	1.709(18)
(Pb1/Bi1)—O2 <sup>i</sup>	2.951(16)	(Ge/V)—O2	1.565(16)
(Pb1/Bi1)—O3 <sup>i</sup>	2.846(15)	(Ge/V)—O3	1.752(15)
(Pb2/Bi2)—O1 <sup>ii</sup>	2.92(3)		
(Pb2/Bi2)—O2 <sup>iii</sup>	2.20(2)		
(Pb2/Bi2)—O3	2.587(15)		
(Pb2/Bi2)—O3 <sup>iv</sup>	2.566(15)		

Symmetry elements (i)  $x^+1, -y^+1,$  and  $-z$ ; (ii)  $x + y, -x,$  and  $-z + 1/2$ ; (iii)  $y + 1, x - y,$  and  $-z + 1/2$ ; and (iv)  $y, -x + y,$  and  $-z$ .

tions from the experimental values are yielded by the incremental Kumok method [26].

#### 4. CONCLUSIONS

The  $\text{Pb}_{10-x}\text{Bi}_x(\text{GeO}_4)_2+x(\text{VO}_4)_{4-x}$  ( $x = 0-3$ ) oxide compounds with an apatite structure were synthesized and their crystal structure was determined for the first time. The high-temperature specific heat was measured by differential scanning calorimetry. It was found that, in the range of 350–900 K, the temperature dependences  $C_p = f(T)$  are described by the Stall–Vestram–Zinke equation. The experimental data were used to calculate the thermodynamic properties of the complex oxides.

**Table 4.** Thermodynamic properties of the  $\text{Pb}_{10-x}\text{Bi}_x(\text{GeO}_4)_2+x(\text{VO}_4)_{4-x}$  ( $x = 1 - 3$ ) apatites

$T, \text{K}$	$C_p, \text{J K}^{-1} \text{mol}^{-1}$	$H^\circ(T) - H^\circ(350 \text{ K}),$ $\text{kJ mol}^{-1}$	$S^\circ(T) - S^\circ(350 \text{ K}),$ $\text{J K}^{-1} \text{mol}^{-1}$	$-\Delta G/T^*, \text{J K}^{-1} \text{mol}^{-1}$
$x = 1$				
350	884.3	—	—	—
400	905.3	44.77	119.5	7.60
450	920.2	90.43	227.1	26.12
500	931.5	136.7	324.6	51.17
550	940.9	183.5	413.9	80.14
600	949.3	230.8	496.1	111.4
650	957.2	278.5	572.4	144.0
700	965.2	326.5	643.6	177.2
750	973.4	375.0	710.5	210.5
800	982.0	423.9	773.6	243.7
850	991.2	473.2	773.6	243.7
900	1000	523.0	890.3	309.2
$x = 2$				
350	895.1	—	—	—
400	921.5	45.46	121.4	7.71
450	940.2	92.02	231.0	26.53
500	954.9	139.4	330.9	52.05
550	967.6	187.5	422.5	81.62
600	979.7	236.2	507.2	113.6
650	991.9	285.4	586.1	146.9
700	1005	335.4	660.1	181.0
750	1019	385.9	729.9	317.2
800	1033	437.2	796.1	249.5
850	1050	489.3	859.2	283.5
900	1068	542.3	919.7	317.2
$x = 3$				
350	910.7	—	—	—
400	938.0	46.25	123.5	7.85
450	959.7	93.70	235.2	27.00
500	978.8	142.2	337.4	53.01
550	996.8	191.6	431.5	83.20
600	1014	241.8	519.0	83.20
650	1033	293.0	600.9	150.1
700	1053	345.2	678.2	185.1
750	1073	398.3	751.5	220.4
800	1095	452.5	821.5	255.8
850	1119	507.9	888.5	291.1
900	1144	564.4	953.2	326.1

\*  $\Delta G/T = [H^\circ(T) - H^\circ(350 \text{ K})]/T - [S^\circ(T) - S^\circ(350 \text{ K})]$ .

#### ACKNOWLEDGMENTS

We are grateful to the Krasnoyarsk Regional Center for Collective Use, Krasnoyarsk Scientific Center, Siberian Branch, Russian Academy of Sciences.

#### FUNDING

The study was carried out under the state assignment for science for the Siberian Federal University, project no. FSRZ-2020-0013.

## CONFLICT OF INTEREST

The authors declare that they have no conflicts of interest.

## REFERENCES

1. T. Yano, Y. Nabeta, and A. Watanabe, *Appl. Phys. Lett.* **18**, 570 (1971).
2. S. A. Ivanov, *Zh. Strukt. Khim* **31**, 80 (1990).
3. M. Gospodinov, *Cryst. Res. Technol.* **25** (3 (K61)) (1990).
4. M. Gospodinov, D. Petrova, P. Sveshtarov, and V. Marinova, *Mater. Res. Bull.* **31**, 1001 (1996).
5. L. Kovács, A. Péter, M. Gospodiniv, and R. Capelletti, *Phys. Status Solidi C* **2**, 689 (2005).
6. E. Chakroun-Ouadhour, R. Ternane, D. Ben Hassan-Chehimi, and M. Trabelsi-Ayadi, *Mater. Res. Bull.* **43**, 2451 (2008).
7. M. Pasero, A. R. Kampf, C. Ferraris, I. V. Pekov, J. Rakovan, and T. J. White, *Eur. J. Miner.* **22**, 163 (2010).
8. F. X. Zhang, M. Lang, J. M. Zhang, Z. Q. Cheng, Z. X. Liu, J. Lian, and R. C. Ewing, *Phys. Rev. B* **85**, 214116 (2012).
9. L. T. Denisova, E. O. Golubeva, N. V. Belousova, V. M. Denisov, and N. A. Galiakhmetova, *Phys. Solid State* **61**, 1343 (2019).
10. S. V. Dobrydnev and M. Yu. Molodtsova, *Izv. TulGU, Estestv. Nauki*, No. 1, 212 (2014).
11. A. V. Ignatov, G. M. Savinkova, E. G. Didorenko, A. Yu. Talykova, E. I. Get'man, and L. V. Pasechnik, *Vestn. Donets. Nats. Univ., Ser. A* **1**, 152 (2014).
12. T. Kanazava, *Inorganic Phosphate Materials* (Nauk. Dumka, Kiev, 1998) [in Russian].
13. V. D. Zhuravlev and Yu. A. Velikodny, *Russ. J. Inorg. Chem.* **54**, 1551 (2009).
14. V. K. Karzhavin, *Thermodynamic Quantities of Chemical Elements. Examples of their Practical Application* (Kol'sk. Nauch. Tsentr RAN, Apatity, 2011) [in Russian].
15. *Bruker AXS TOPAS V4: General Profile and Structure Analysis Software for Powder Diffraction Data, User's Manual* (Bruker AXS, Karlsruhe, Germany, 2008).
16. L. T. Denisova, L. A. Irtyugo, Yu. F. Kargin, V. V. Beletskii, and V. M. Denisov, *Inorg. Mater.* **53**, 93 (2017).
17. S. A. Ivanov and V. E. Zavodnik, *Sov. Phys. Crystallogr.* **34**, 493 (1989).
18. L. T. Denisova, Yu. F. Kargin, E. O. Golubeva, N. V. Belousova, and V. M. Denisov, *Inorg. Mater.* **55**, 162 (2019).
19. D. Stall, E. Westram, and G. Zinke, *Chemical Thermodynamics of Organic Compounds* (Wiley, New York, 1969).
20. C. G. Maier and K. K. Kelley, *J. Am. Chem. Soc.* **54**, 3243 (1932).
21. L. T. Denisova, A. D. Izotov, Yu. F. Kargin, V. M. Denisov, and N. A. Galiakhmetova, *Dokl. Phys. Chem.* **62**, 205 (2017).
22. L. F. Reznitskii, *Solid State Calorimetry: Structural, Magnetic, Electronic Transformations* (Mosk. Gos. Univ., Moscow, 1981) [in Russian].
23. G. K. Moiseev, N. A. Vatolin, L. A. Marshuk, and N. I. Il'inykh, *Temperature Dependences of the Reduced Gibbs Energy of Some Inorganic Substances (Alternative Data Bank ASTRA.OWN)* (Ural. Otdel. RAN, Yekaterinburg, 1997) [in Russian].
24. J. Leitner, P. Chuchvalec, D. Sedmidubský, A. Strejc, and P. Abrman, *Thermochim. Acta* **395**, 27 (2003).
25. J. Laitner, P. Voňka, D. Sedmidubský, and P. Svoboda, *Thermochim. Acta* **497**, 7 (2010).
26. V. N. Kumok, *Direct and Inverse Problems of Chemical Thermodynamics* (Nauka, Novosibirsk, 1987), p. 108 [in Russian].

Translated by E. Bondareva